AIAA 79-1481R

Quantitative Predictions of Dump Combustor Flowfields

Hermann Viets*
Wright State University, Dayton, Ohio
and
James E. Drewry†
Air Force Aero Propulsion Laboratory, Wright-Patterson AFB, Ohio

An approximate solution is proposed for a coaxial dump combustor flowfield. The core region of the flow is treated with the recirculation region shape specified. The problem is thereby reduced to a set of parabolic differential equations. The core region is then divided into a number of streamtubes. This reduces the governing equations to a set of simultaneous algebraic equations which are much simpler to solve. Comparisons with experimental data are presented.

Nomenclature

A = area
C_i = concentration of the ith component
C_p = specific heat
D = inlet diameter
$\mathfrak{D}$ = diffusion coefficient
K = coefficient in eddy viscosity
k = thermal conductivity
M = molecular weight
$\dot{m}$ = mass transfer rate
P = pressure
q = heat transfer
q_{gen} = heat generated
q_m = heat transfer associated with mass
r = radius
R = gas constant
T = temperature
T_b = boiling temperature at 1 atm
V = velocity
w = diffusion velocity
x = mass fraction
X = length in streamwise direction
ϵ = eddy viscosity
π = 3.1415
ρ = density
τ = shear stress
χ = mole fraction
Σ = sum
Δ = change

Subscripts

C_L = centerline
d = downstream
i = inside
mix = gas mixture
n = nth streamtube value
o = outside
u = upstream
w = wall

Presented as Paper 79-1481 at the AIAA 12th Fluid and Plasma Dynamics Conference, Williamsburg, Va., July 23-25, 1979; submitted Sept. 4, 1979; revision received May 27, 1980.

*Professor. Associate Fellow AIAA.
†Senior Research Engineer (presently Director, Energy Conservation Research, Gas Research Institute, Chicago, Ill.). Member AIAA.

Introduction

IN the analysis of coaxial dump combustors as applied to integral rocket ramjets, the main objective is to predict the performance of such an arrangement by determining the general flowfield including all of the fluid dynamic effects as well as combustion. The flowfield in a typical coaxial ramjet dump combustor, shown in Fig. 1, has been investigated experimentally by Drewry[1,2] and Abbott and Kline[3] among others. In spite of the simplicity of the geometry, the actual numerical prediction of the flowfield is a rather complicated affair. This difficulty is caused by the fact that the fluid is nonhomogeneous since it contains fuel, air, and combustion products. In addition, the flow has strong velocity and temperature gradients and a closed recirculation region which requires that the general governing equations be of elliptical form. And, as though this were not enough, the actual fluid properties are not known accurately, so that the eddy viscosity, for example, is not a simple function of the local properties. With additional effort, the viscous effects can be handled, for example, by the turbulent kinetic energy (TKE) method. Additional difficulties arise when the other required fluid properties, conductivity and specific heat, are considered.

The approximate solution proposed by the present analysis is to treat the core region with the exception of the recirculation region. In this way, the problem is simplified since the core flow region may be treated by a set of parabolic equations (i.e., the boundary-layer equations) and the solution obtained by a simple marching technique. An additional simplification is that the partial differential equations are not solved directly but rather the problem is set up as a number of streamtubes and the equations written for each of the tubes. This simplification results in a set of simultaneous algebraic equations which are, of course, much simpler to solve than simultaneous partial differential equations.

General Equations

As mentioned above, the analysis is concerned with the solution of algebraic equations as related to a number of streamtubes. The matching conditions at the interface between two streamtubes are that the heat transfer out of one streamtube is equal to the heat transfer into the adjoining tube and that the shear on one tube is numerically equal in magnitude and opposite in sign to that on the next tube.

A general annular streamtube is shown in Fig. 2. The radius from the center of the duct is indicated, as are the upstream and downstream pressures and the inner and outer values of heat transfer and shear. The governing equations are discussed in the following paragraphs.

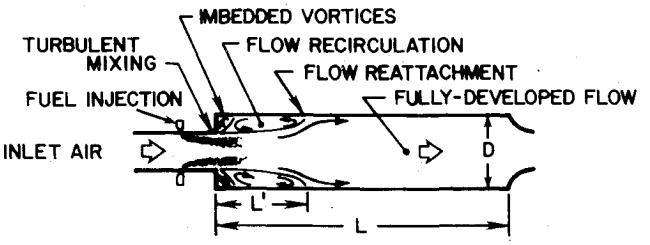

Fig. 1 Typical ramjet dump combustor.

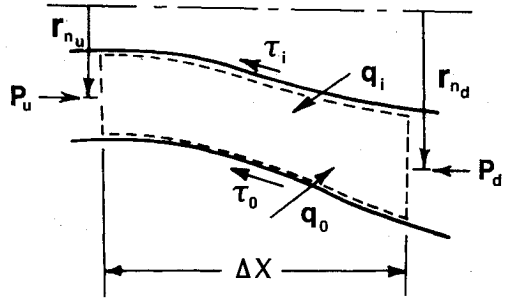

Fig. 2 Streamtube geometry.

Conservation of Mass

$$\rho_{d_n} V_{d_n} A_{d_n} - \rho_{u_n} V_{u_n} A_{u_n} = 0 \tag{1}$$

This is true for the overall mass flow within the streamtube by definition. However, it is not necessarily true for each of the species within the streamtube because a small amount of mass transfer will be allowed across the interface due to diffusion and mixing. Perhaps a better term would be mass *exchange* across the interface because the total amount of mass within each streamtube is conserved. There is, of course, the implicit assumption that the specie velocity across the interface is neglegibly small so that the overall flow system in Fig. 2 is unaffected.

Conservation of Momentum

The streamtube flow is one-dimensional so the pressure is constant across all streamtubes (i.e., $\partial P/\partial r = 0$). The total force on the control volume in Fig. 2 is caused by the pressure on the boundaries of the tube as well as the shear forces on the sides of the tube. Then

$$P_{u_n} A_{u_n} - P_{d_n} A_{d_n} - \tau_{i_n} A_{i_n} - \tau_{o_n} A_{o_n} + \frac{(P_{u_n} + P_{d_n})}{2} (A_{d_n} - A_{u_n})$$
$$= \rho_{d_n} V_{u_n}^2 A_{d_n} - \rho_{u_n} V_{u_n}^2 A_{u_n} \tag{2}$$

where

$$A_{i_n} = 2\pi r_{i_n} \Delta X$$
$$A_{o_n} = 2\pi r_{o_n} \Delta X$$

Conservation of Energy

Since the analysis is eventually aimed at a treatment of a reacting system, allowance must be made for a heat generation term, q_{gen}. This term would be determined by an examination of the combustion kinetics of the problem or by a semiempirical postulation of the rates of reaction. In addition, there is a heat transfer associated with the transfer (or exchange) of mass across the streamtubes, q_{mn}. Then

$$C_{p_n} T_{d_n} + \frac{V_{d_n}^2}{2} - \left(C_{p_n} T_{u_n} + \frac{V_{u_n}^2}{2} \right) = q_{\text{gen}} + q_{i_n} + q_{o_n} + q_{m_n} \tag{3}$$

The specific heats C_{p_n} must be determined from the constituents of the flow and will, in general, be different for each streamtube.

Equation of State

$$P = \rho R T$$

$$\frac{P}{\rho T} = R = \frac{\hat{R}}{M} = \text{universal gas constant/molecular weight} \tag{4}$$

The molecular weight of the mixture in each streamtube may, in general, change with chemical reaction and/or mixing across streamtubes, thus

$$\frac{P_{u_n} M_{u_n}}{\rho_{u_n} T_{u_n}} = \frac{P_{d_n} M_{d_n}}{\rho_{d_n} T_{d_n}} = \hat{R} = \text{constant} \tag{5}$$

where the molecular weight of the flow in each streamtube may be found from its constituents by[5]

$$M = \sum_k M_k \chi_k \tag{6}$$

where

$$\chi_k = \text{mole fraction} = \frac{\text{moles}_k}{\text{total moles}} \tag{7}$$

The relation between the mole fraction χ_k and the mass fraction is

$$\chi_k = \frac{\text{mass}_k}{M_k} \Big/ \sum_k \frac{\text{mass}_k}{M_k} \tag{8}$$

so

$$M = \text{mass}_{\text{total}} \Big/ \left[\sum_k \left(\frac{\text{mass}_k}{M_k} \right) \right] \tag{9}$$

but the $\text{mass}_{\text{total}}$ is conserved within the streamtube so the final equation of state is

$$P_{d_n} \Big/ \left[\rho_{d_n} T_{d_n} \left(\sum_k \frac{\text{mass}_k}{M_k} \right)_{d_n} \right] = P_{u_n} \Big/ \left[\rho_{u_n} T_{u_n} \left(\sum_k \frac{\text{mass}_k}{M_k} \right)_{u_n} \right] \tag{10}$$

Therefore, in conclusion, there are four equations [Eqs. (1-3) and (10)] and five unknowns (P, A, V, ρ, T) for each streamtube. The additional required equation arises from the geometrical constraints of the duct and the fact that a lateral pressure variation is not permitted.

In principle then, the pressure may be imposed as an initial guess at the solution, the calculation of the variables performed, and the areas summed to see if the required flow area is equal to the available geometrical area. If it is, the solution is valid. If the areas do not match, the calculation must be repeated with a different assumption for the downstream pressure.

Detailed Modeling

Heat Transfer

The heat-transfer methods considered in the program are conductive and convective heat transfer. It would be possible to consider radiant heat transfer as an additional term in the future.

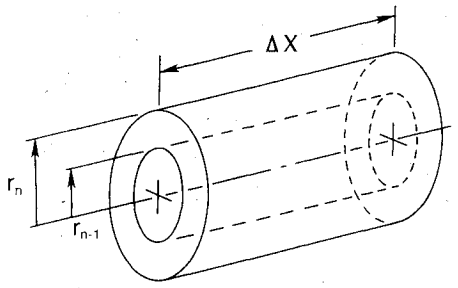

Fig. 3 Annular streamtube segment.

The conductive heat transfer through a cylindrical surface of length ΔX and radius r is:

$$q = -k2\pi r\Delta X\frac{dT}{dr} \tag{11}$$

For an annular segment, it can be seen from Fig. 3 that

$$q_{o_n} = -4k\pi r_n\Delta X(T_{n+1}-T_n)/(r_{n+1}-r_{n-1}) \tag{12}$$

where k is the thermal conductivity of the gas mixture. For a mixture of reactive gases, the determination of the thermal conductivity is rather complicated[6] and, in view of the approximations made in other portions of the analysis, probably needlessly so. The thermal conductivity will therefore be determined by employing the method for the thermal conductivity of mixtures of inert gases and, in particular, by employing the equation recommended for mixtures of di- and polyatomic gases.[6]

$$k_{\text{mix}} = \sum_{i=1}^{n} k_i\Big/\left[1+\frac{1}{\chi_i}\sum_{\substack{j=1\\ j\neq i}}^{n} B_{ij}\chi_j\right] \tag{13}$$

where B_{ij} is found from (for example, $B_{ij}=B_{12}$)

$$B_{12}=\frac{1}{4}\left\{1+\left[\frac{\mu_1}{\mu_2}\left(\frac{M_2}{M_1}\right)^{3/4}\frac{(1+S_1/T)}{(1+S_2/T)}\right]^{1/2}\right\}^2\frac{(1+S_{12}/T)}{(1+S_1/T)} \tag{14}$$

where

$$\frac{\mu_1}{\mu_2}=\frac{k_1(C_{p_2}+1.25R/M_2)}{k_2(C_{p_1}+1.25R/M_1)} \tag{15}$$

Here S of each of the gases is determined from their absolute boiling temperatures T_b at 1 atm

$$S=1.5T_b \tag{16}$$

while

$$S_{12}=\sqrt{S_1S_2} \tag{17}$$

except for gases containing water vapor or ammonia, in which case

$$S_{12}=0.733\sqrt{S_1S_2} \tag{18}$$

Specific Heats

The specific heats of the gases are functions of temperature and may be found in Appendix A of Van Wylen and Sonntag.[7] For example, the specific heat of oxygen for a temperature range of 300-3500 K is

$$C_{p_{o_2}}=37.432+0.020102\theta^{1.5}-178.57\theta^{-1.5}+236.88\theta^{-2} \tag{19}$$

where $\theta=T$ (Kelvin)/100 and the specific heat has units of kJ/kg-mole·K.

In addition, the average specific heat is required for each streamtube and is found by a mass average (see Ref. 5, p. 168)

$$C_{p_{\text{av}}}=\sum_{j=1}^{n} x_jC_{p_j} \tag{20}$$

Mass Exchange

By definition, there is no mass transfer across a streamline because there can be no velocity component normal to the streamline. However, the concept of a streamline originates from a laminar flow view of fluid mechanics. In turbulent flow the streamline is defined in terms of the time average of the turbulent flow component of velocity relative to the streamline, but this component averages out to zero with time. However, there may be a net transfer of mass of particular constituents while the overall mass transfer is zero. This transfer of mass may occur due to diffusion across the streamline or to the turbulence structure.

The diffusion velocity is governed by the concentration gradient normal to the streamline

$$w=-\mathfrak{D}\frac{\partial c}{\partial y} \tag{21}$$

where $\mathfrak{D}$ is the diffusion coefficient which depends upon both the properties of fluid which is diffusing and the properties of the medium into which the diffusion is taking place. Numerical values are chosen from Eckert,[8] either directly or extrapolated from those results given.

The numerical values employed in this analysis are, of course, only approximations in the sense that the available values are generally for a two-component system. Thus, it is necessary to assume some effective behavior for the rest of the gaseous system into which a single component diffuses. For example, to model the diffusion of the oxygen component, the rest of the system is treated as being equivalent to nitrogen.

For the diffusion of nitrogen into the gaseous mixture, the mixture is treated as oxygen. Then the same diffusion coefficient can be used as for the diffusion of oxygen into nitrogen by the reasoning presented in Ref. 9. Estimates of the unknown diffusion coefficients may be made by noting that the heavier gases diffuse more slowly than the lighter gases.

Mass Exchange by Turbulent Mixing

In addition to the exchange of mass across the streamlines by diffusion, mass may also be exchanged by turbulent mixing at the streamline. This is due to the fact that in the case of a turbulent flow there are random excursions of the particles from their time-averaged path (i.e., from the streamlines). These random motions lead to an exchange of mass between various streamtubes. Unfortunately, no empirical data seem to be available to allow the determination of the degree to which this effect is important.

The effect of large-scale motions on the mixing of turbulent flows has been recognized only relatively recently.[10] Investigations of this effect and also that of the flows' level of turbulent intensity are expected to yield very useful empirical data in the next several years.

In the meantime, without the required empirical information, a relation for the mass transfer due to the turbulence structure can be produced in a phenomenological fashion. Since the mass transfer is produced by the mixing, it is expected that the mass transfer should be proportional to the eddy viscosity and the velocity gradient. Therefore, in this very simplistic view, the mass transfer is proportional to the shearing stress,

$$\dot{m}_{\text{turb}}\sim\tau \tag{22}$$

where

$$\tau=\rho\epsilon\frac{\partial u}{\partial y} \tag{23}$$

The eddy viscosity modeling is, however, a laminarization of the turbulent mixing so it does not explicitly reflect the large-scale turbulent structure. The effect of this turbulent structure must be implicit in the magnitude of ϵ as a function of position.

Eddy Viscosity Formulation

In keeping with the spirit of the present analysis, only very simple eddy viscosity models will be considered. It would be especially useful if the model were one-dimensional so that no radial variation of eddy viscosity need be considered. The model finally employed is an adaptation of one originally due to Prandtl and has been shown to be useful in the prediction of velocity and temperature decays in axisymmetric jets with and without coflowing streams.[11,12] The form of model is

$$\rho\epsilon=K\mathfrak{L}[(\rho u)_{C_L}-(\rho u)_{\text{wall}}] \tag{24}$$

where $\mathfrak{L}$ is the mixing length equal to the radius of the core flow. The coefficient K is to be determined from empirical data obtained from one dump combustor geometry. Predictions will then be made for other geometries and these will be compared to experimental results.

Chemical Reaction

According to Edelman and Harsha,[13] the controlling reaction for the combustion of the hydrocarbons being considered here is the partial oxidation

$$C_nH_m+n/2O_2\rightarrow m/2\ H_2+nCO \tag{25}$$

with an empirical reaction rate of

$$\frac{5.52\times10^{-8}}{p^{0.825}}(C_{C_nH_m})^{1/2}(C_{O_2})Te^{(12{,}200/T)}\ \frac{g\text{fuel}}{\text{cm}^3\text{s}} \tag{26}$$

where p = pressure in atmospheres

$$(C_{C_nH_m}),(C_{O_2})\equiv\text{molar concentrations of } C_nH_m, O_2 \tag{27}$$

$$T=\text{temperature K}$$

For a constant pressure or steady flow process, the heat generated by the combustion process is,

$$\text{heat of reaction} = -\text{enthalpy of combustion}$$

where the enthalpy of combustion may be found in Ref. 7.

Using the above empirical reaction rate, the problem reduces to that of precisely determining the concentrations of fuel and oxidizer in the reaction zone. That is the problem treated by the present analysis, along with a prediction of the local velocity and temperature distributions.

Recirculation Boundary Condition

The present analysis considers only the main or core flow. It does not attempt to compute the flow in the recirculation region. Thus, the shape of the recirculation region is required as an input into the present analysis. As a result of analyzing the data in Refs. 1 and 2, the shape chosen was a quasielliptical recirculation region. The additional interaction of the core flow with the recirculation region is through the velocity boundary condition and the amount of heat and mass transfer from the separated flow to the core flow. The velocity boundary condition is specified as a percentage of the centerline velocity.

Numerical Predictions

The most revealing single parameter in the dump combustor case is the axial pressure distribution in the duct. Therefore, the duct pressure distribution is the primary target for a match between the analysis and the available experimental results. Once such a match is achieved, the next parametric comparison is between the predicted and experimentally observed velocity distribution. Of course, any changes made to predict the velocity more accurately will clearly have an effect on the pressure distribution and therefore the attempt is a repetitive process. The primary mechanisms considered for these changes are the shape of the recirculation region, the dependence of the eddy viscosity on fluid properties and position, and the boundary conditions on the velocity at the interface between the recirculation region and the main flow.

Effect of Recirculation Region Shape

A rather consistent result observed in numerous investigations of rearward-facing steps is the "dip" or decrease in static pressure immediately downstream of the corner as shown in Fig. 4. This pressure reduction can be explained simply by noting the effect of changes in the shape of the recirculation region. Flow through a channel results in an increasing boundary-layer thickness, leading to an increased displacement thickness. Thus, the flow outside the boundary layer must be accelerated to allow for a constant mass flow rate passing any streamwise station. The mechanism to achieve this is a reduction in the static pressure with streamwise distance.

Now consider the main flow immediately after it has separated from the corner of the dump station, shown schematically in Fig. 5. Although the solid wall is no longer there, a retarding shear still exists because the fluid in the recirculation region is at much lower velocity than the high-velocity main flow. If then the assumed shape of the recirculation region continues as an extension of the upstream wall (i.e., no diffusion of the main flow), the pressure will drop by the mechanism discussed above. Changing the shape of the assumed recirculation region, so that there is an expansion of the main flow area to allow for a growth in the displacement

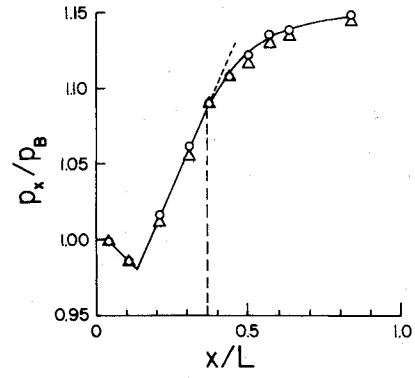

Fig. 4 Typical static pressure.

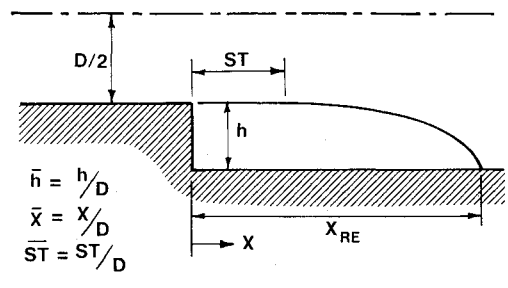

Fig. 5 Geometry of recirculation region.

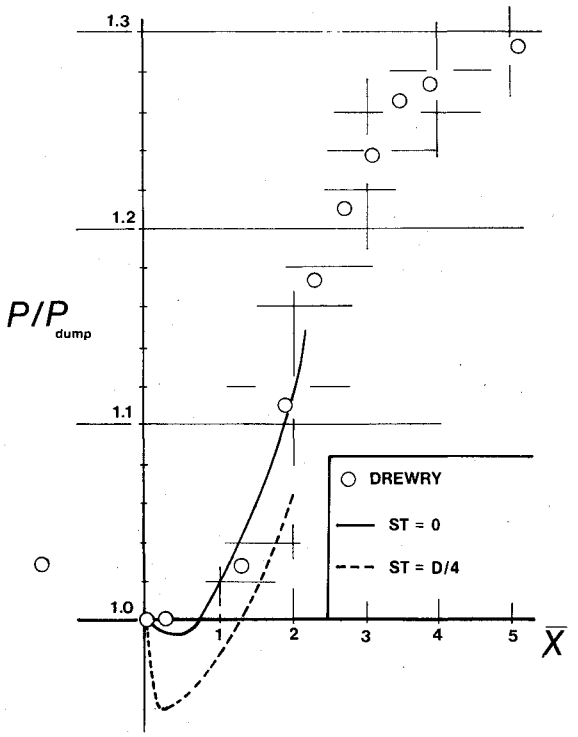

Fig. 6 Effect of recirculation region shape on pressure.

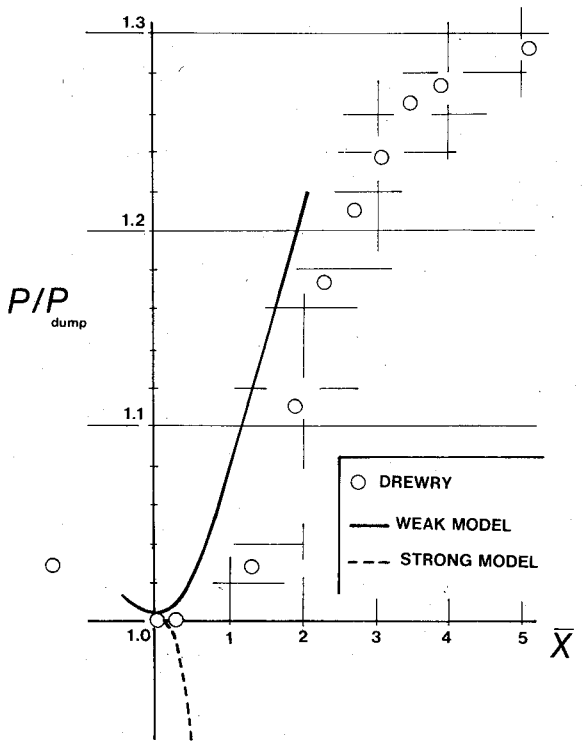

Fig. 7 Effect of eddy viscosity strength.

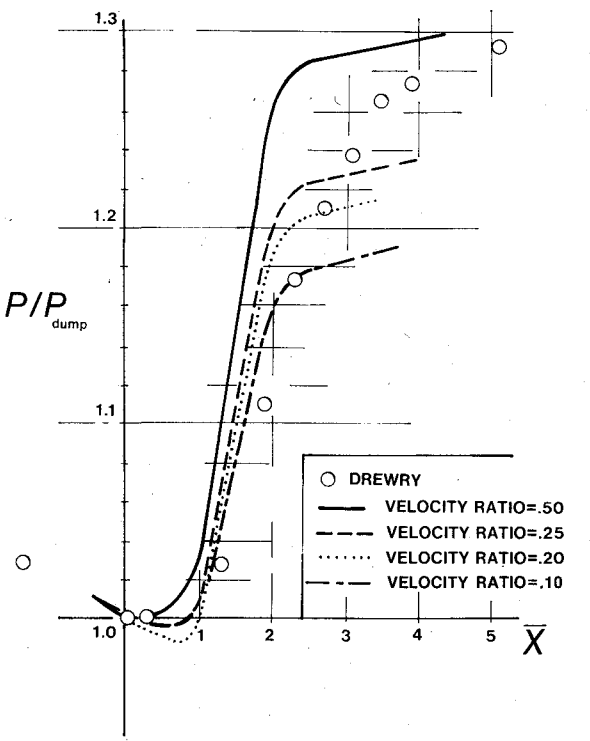

Fig. 8 Effect of recirculation velocity boundary condition on pressure.

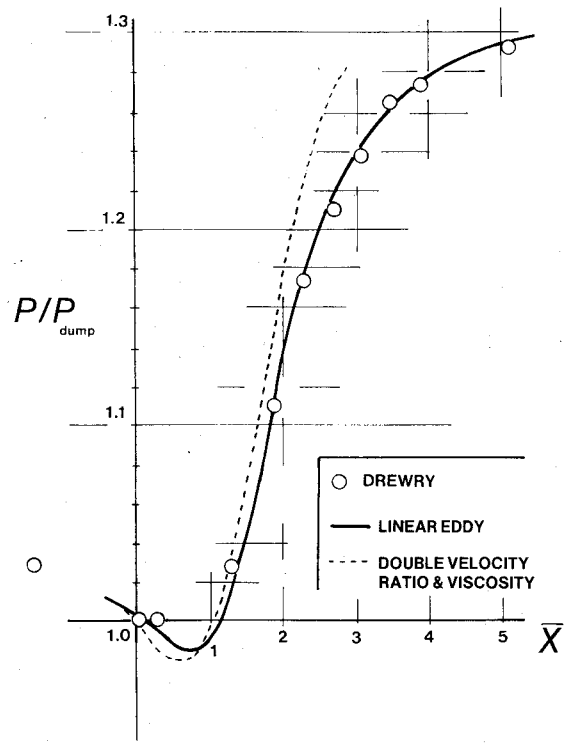

Fig. 9 Best pressure match and effect of adjustment to improve velocity profile prediction, $D = 6.35$ cm, $k = 0.00025$.

thickness, results in a smaller reduction in the pressure immediately downstream of the corner. This effect may be seen in Fig. 6 compared to the experimental pressure distribution. Each pressure distribution is computed using the same inlet data and assumed eddy viscosity. The only difference is the shape of the recirculation region.

The parameters involved in the specification of the recirculation region shape are shown in Fig. 5, where the length ST refers to the straight portion of the recirculation region.

Effect of Eddy Viscosity on Pressure

The previously described effect of the recirculation shape can be emphasized by the choice of an eddy viscosity model. That is, a strong eddy viscosity will exaggerate the effect of shape, while a weak model will render the shape relatively unimportant because the growth of the displacement thickness will be slow. An extreme example of this is shown in Fig. 7. In each case the calculation is started at a position $\bar{x} = -0.48$,

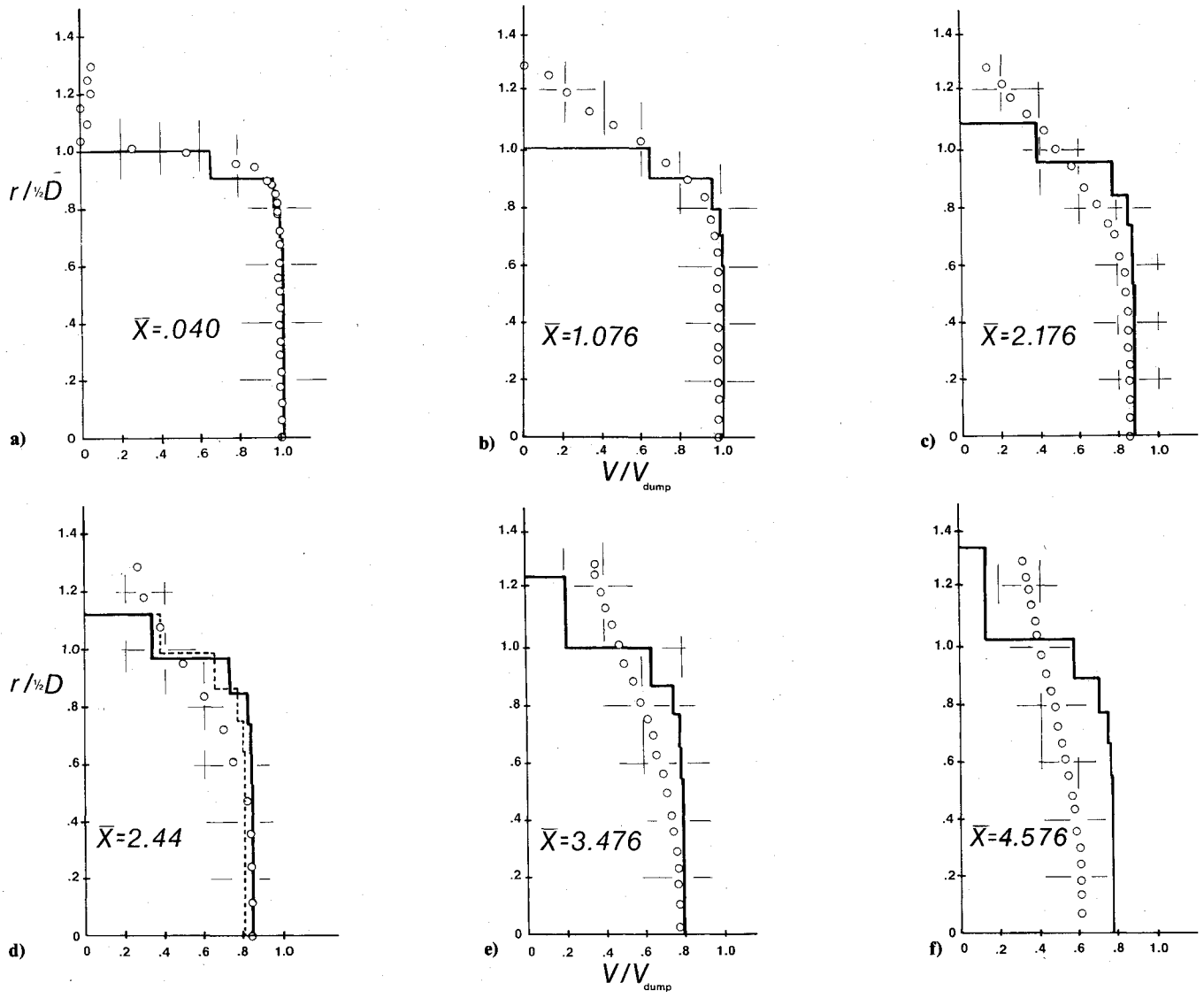

Fig. 10 Quantitative comparison of computed velocity profiles (based upon best match of Fig. 9) with experimental data of Ref. 1.

upstream of the dump station. The strong eddy viscosity model has a streamwise dependence which increases 30 times as fast as the weak model. Thus, the strong model results in a rapid growth of the displacement thickness and hence a rapid pressure reduction. In each case there is an immediate diffusion (ST = 0) of the flow at the corner.

Effect of the Velocity Boundary Condition

As mentioned above, there is a shear exerted on the main flow at its interface with the recirculation region due to the velocity difference between the two regions. If this velocity difference is specified by the ratio of the recirculation zone velocity to the main flow velocity at the interface, the results shown in Fig. 8 are obtained. The geometry consists of a moderate straight section ST = 0.72. The only difference between the various computations is the shear velocity ratio which varies between 0.1 and 0.5. For lower velocity ratios, the shear is increased. Increasing shear results in a more rapid boundary-layer growth and thus a faster displacement thickness increase and increased tendency for pressure reduction. Thus the pressure increase due to diffusion is terminated at a lower value in the case of increased shear (lower velocity ratios).

Effect of Eddy Viscosity on Velocity Profiles

The most successful comparison of predicted to experimentally determined pressure distributions obtained in this study is shown in Fig. 9. In this case the eddy viscosity dependence is linear with streamwise distance, $K = 0.00025$, and the straight portion of the recirculation zone is ST = 0.72. The modeling of the velocity difference across the recirculation zone boundary allows a linear increase in the recirculation zone velocity until it equals 45% of the freestream velocity, and then allows a linear decrease in its velocity to account for the observation that it goes to zero at the end of the recirculation zone. The empirically determined models have forced this match, of course, and the actual test of its accuracy is by comparison to a somewhat different velocity or geometry. Predictions of other geometries will be presented, as will a discussion of the dashed curve in Fig. 9.

The velocity profiles, predicted and experimental, are presented in Fig. 10 for various streamwise stations corresponding to the solid pressure distribution curve in Fig. 9. The computation is begun at a station $\bar{x} = -0.48$ and the comparison at essentially the dump station $\bar{x} = 0.04$ is reasonable. As the streamwise distance increases, the experimental velocity profile expands. The numerical predictions are for only the main flow, so the "tail" of the measured profile is not predicted since it is in the recirculation zone. The stepwise nature of the predicted profiles is due to the fact that the velocity is constant within any streamtube.

As the streamwise distance increases, it is apparent that the outer streamtube velocity becomes too low, while most of the remaining streamtubes contain velocities which are too high.

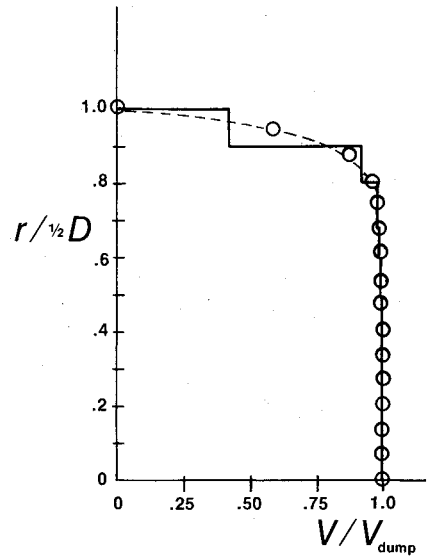

Fig. 11a Measured inlet velocity profile and input velocity profile for calculations, $D = 5.08$ cm (data due to Boray[14]).

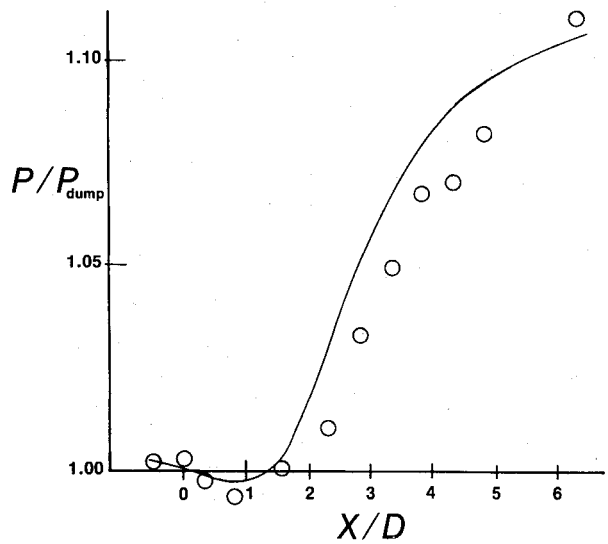

Fig. 11b Resulting streamwise pressure distribution for $D = 5.08$ cm employing same models as Fig. 9, $D = 6.35$ cm (see Boray[14]).

The streamtubes near the center predict a rather accurate velocity, which is really a reflection of the fact that the pressure distribution is quite accurate, as seen in Fig. 9. The overall indication, then, is that the shear produced by the interaction with the recirculation region is too great (resulting in a low velocity in the outermost streamtube) and the eddy viscosity is too low (resulting in a slow diffusion of the momentum loss at the boundary).

In order to counteract these effects, the shear at the boundary is reduced by doubling the ratio of recirculation flow velocity to main velocity. Additionally, the eddy viscosity coefficient is doubled. As seen by the dashed curve in Fig. 10d, the result is as expected. The reduced shear results in an increased velocity in the outer streamtube, while the increased eddy viscosity reduces the velocity of the profile. These changes certainly produce an improvement in the velocity predictions. However, their effect on the pressure distribution is shown in Fig. 9. The double-shear/double-eddy viscosity curve may be seen to have a very significant deviation from the empirical pressure distribution. Thus, changing the mixing rate has had a strong effect on the displacement thickness and, in turn, on the pressure

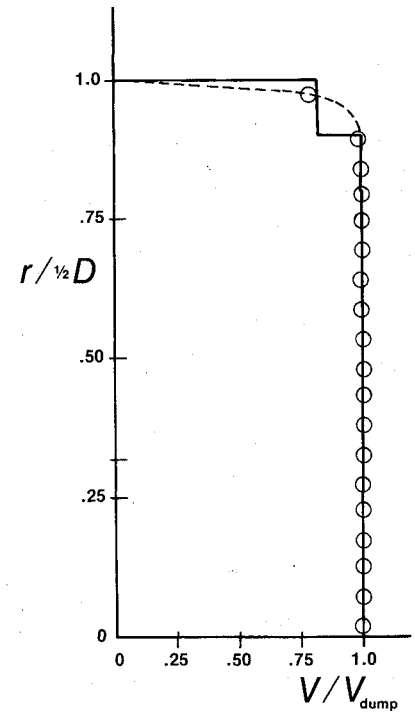

Fig. 12a Measured inlet velocity profile and input velocity profile for calculations, $D = 7.62$ cm (see Boray[14]).

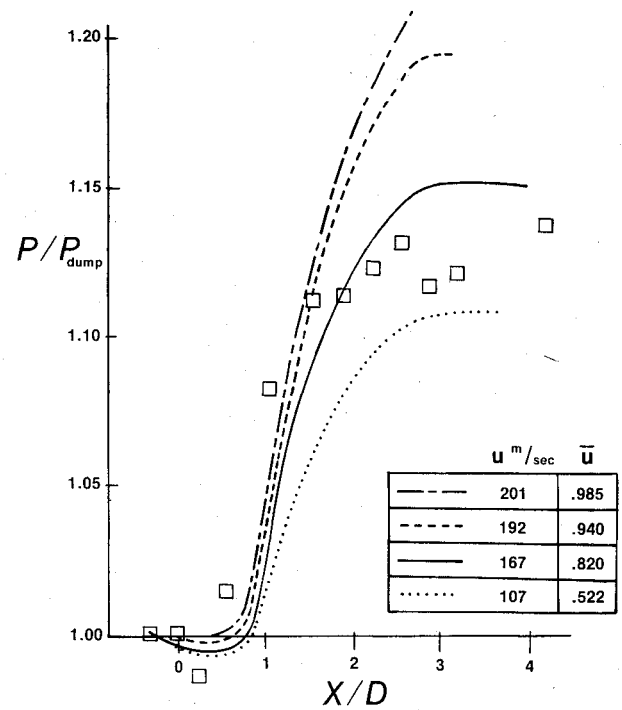

Fig. 12b Resulting streamwise pressure distribution for $D = 7.62$ cm employing same models as Fig. 9, $D = 6.35$ (see Boray[14]).

distribution. Further changes may therefore be made in order to obtain a better prediction of both pressure and velocity distribution.

Comparisons with Other Geometries

The actual confrontations with experimental data, to this point, have employed the results of Ref. 1 for an inlet size $D = 6.35$ cm. In order to test the usefulness of the predictions for various sizes, calculations have been performed for two other sets of data[14] for inlet diameters of 5.08 and 7.62 cm (2 and 3 in.).

The measured inlet profile at the dump station for the former case, $D = 5.08$ cm, is shown in Fig. 11a, along with the shape of the inlet profile to calculations. The inlet temperature profile was practically constant at 250 K (450°R) except near the wall where is rose to 265 K (478°R). The eddy viscosity variation [Eq. (24)], developed by comparison to the data for $D = 6.35$ cm (see Fig. 9), is employed without any modification to calculate the dump combustion flowfield. The modeling of the recirculation length, diffusion coefficients, thermal conductivities, specific heats, and mass exchange remains precisely as in the previous case. The only change is in the inlet conditions and the geometry.

The resulting comparison between the predicted and experimental streamwise pressure distribution for $D = 5.08$ cm is shown in Fig. 11b. The calculated variation shows all the characteristics of the experimental results, including the pressure decrease after the corner, and the quantitative comparison is quite reasonable.

The inlet velocity profile for a larger inlet diameter, $D = 7.62$ cm, is shown in Fig. 12a. Actually, the profile is taken 0.25 cm downstream from the corner so the boundary layer is probably slightly fuller than it is precisely at the corner. The velocities in the corresponding ten streamtubes are also shown. The streamwise pressure distribution resulting from this inlet profile is shown in Fig. 12b as the solid curve. It may be seen that the streamwise pressure rise is reasonably well predicted by the calculation. It is of particular interest to observe the strong influence of the inlet velocity on the pressure distribution. The velocity in the outer streamtube, divided by the centerline value, is designated as $\bar{u}$. A nearly uniform velocity distribution results in a larger pressure rise, while a more fully developed boundary layer reduces the resulting downstream pressure. This result underscores the importance of having an accurate assessment of the inlet conditions to the dump combustor geometry.

Conclusions

The above analysis and results show that a simplified view of the complex flow problem in a dump combustor offers the potential of a design tool without the complexity of solving the full equations. The trends observed in the numerical results are explained by physical reasoning and the comparison between predictions and experiment for three different combustor sizes shows quite reasonable agreement.

Acknowledgments

This work was conducted under the auspices of the Air Force Aero Propulsion Laboratory Senior Investigator Program, Contract F33615-77-C-2069 (University of Dayton).

References

[1] Drewry, J. E., "Fluid Dynamic Characterization of Sudden-Expansion Ramjet Combustor Flowfields," *AIAA Journal*, Vol. 16, April 1978, pp. 313-319.

[2] Drewry, J. E., "Characterization of Sudden-Expansion Dump Combustor Flowfields," Air Force Aero Propulsion Laboratory Rept. TR-76-52, July 1976.

[3] Abbott, D. E. and Kline, S. J., "Experimental Investigation of Subsonic Turbulent Flow Over Single and Double Backward Facing Steps," *Journal of Basic Engineering*, Sept. 1962, pp. 317-325.

[4] Harsha, P. T., "Kinetic Energy Methods," *Handbook of Turbulence*, Vol. 1, edited by W. Frost and T. Moulden, Plenum Publishing Corp., 1977, Chap. 8.

[5] Penner, S. S., *Chemistry Problems in Jet Propulsion*, Pergamon Press, 1957, p. 135.

[6] Tsederberg, N. V., *Thermal Conductivity of Gases and Liquids*, MIT Press, Cambridge, Mass., 1965.

[7] Van Wylen, G. J., and Sonntag, R. E., *Fundamentals of Classical Thermodynamics*, John Wiley & Sons, New York.

[8] Eckert, E.R.G., *Introduction to the Transfer Heat and Mass*, McGraw-Hill Book Co., New York, 1950.

[9] Viets, H. and Drewry, J. E., "Quantitative Predictions of Dump Combustor Flowfields," AIAA Paper 79-1481, July 1979.

[10] Brown, G. and Roshko, A., "On Density Effects and Large Structure in Turbulent Mixing Layers," *Journal of Fluid Mechanics*, Vol. 64, 1971, pp. 775-816.

[11] Viets, H., "Prandtl Eddy Viscosity Model for Coaxial Jets," *AIAA Journal*, Vol. 10, Dec. 1972, pp. 1684-1685.

[12] Boyle, R. E. and Viets, H., "Eddy Viscosity Model for Variable Density Coflowing Streams," *Journal of Aircraft*, Vol. 11, Dec. 1974, pp. 721-722.

[13] Edelman, R. B. and Harsha, P. T., "Application of Modular Modeling to Ramjet Performance Prediction," AIAA Paper 78-944, July 1978.

[14] Boray, R. S., "Flowfield Studies of Dump Combustors," Paper presented at 16th JANNAF Combustion Meeting, Monterey, Calif., Sept. 1979.